Publication Year	2022
Acceptance in OA	2025-03-08T17:58:16Z
Title	The MeerKAT Galaxy Cluster Legacy Survey: I. Survey Overview and Highlights
Authors	Knowles, K., Cotton, W. D., Rudnick, L., Camilo, F., Goedhart, S., Deane, R., RAMATSOKU, MPATI ANALICIA, Bietenholz, M. F., Brüggen, M., Button, C., Chen, H., Chibueze, J. O., Clarke, T. E., DE GASPERIN, Francesco, Ianjamasimanana, R., Józsa, G. I.G., Hilton, M., Kesebonye, K. C., Kolokythas, K., Kraan-Korteweg, R. C., Lawrie, G., Lochner, M., Loubser, S. I., Marchegiani, P., Mhlahlo, N., Moodley, K., Murphy, E., Namumba, B., Oozeer, N., Parekh, V., Pillay, D. S., Passmoor, S. S., Ramaila, A. J.T., Ranchod, S., Retana-Montenegro, E., Sebokolodi, L., Sikhosana, S. P., Smirnov, O., Thorat, K., VENTURI, Tiziana, Abbott, T. D., Adam, R. M., Adams, G., Aldera, M. A., Bauermeister, E. F., Bennett, T. G.H., Bode, W. A., Botha, D. H., Botha, A. G., Brederode, L. R.S., Buchner, S., Burger, J. P., Cheetham, T., De Villiers, D. I.L., Dikgale-Mahlakoana, M. A., Du Toit, L. J., Esterhuyse, S. W.P., Fadana, G., Fanaroff, B. L., Fataar, S., Foley, A. R., Fourie, D. J., Frank, B. S., Gamatham, R. R.G., Gatsi, T. G., Geyer, M., Gouws, M., Gumede, S. C., Heywood, I., Hlakola, M. J., Hokwana, A., Hoosen, S. W., Horn, D. M., Horrell, J. M.G., Hugo, B. V., Isaacson, A. R., Jonas, J. L., Jordaan, J. D.B., Joubert, A. F., Julie, R. P.M., Kapp, F. B., Kasper, V. A., Kenyon, J. S., Kotzé, P. P.A., Kotze, A. G., Kriek, N., Kriel, H., Krishnan, V. K., Kusel, T. W., Legodi, L. S., Lehmensiek, R., Liebenberg, D., Lord, R. T., Lunsky, B. M., Madisa, K., Magnus, L. G., Main, J. P.L., Makhaba, A., Makhathini, S., Malan, J. A.
Publisher's version (DOI)	10.1051/0004-6361/202141488
Handle	http://hdl.handle.net/20.500.12386/36550
Journal	ASTRONOMY & ASTROPHYSICS
Volume	657

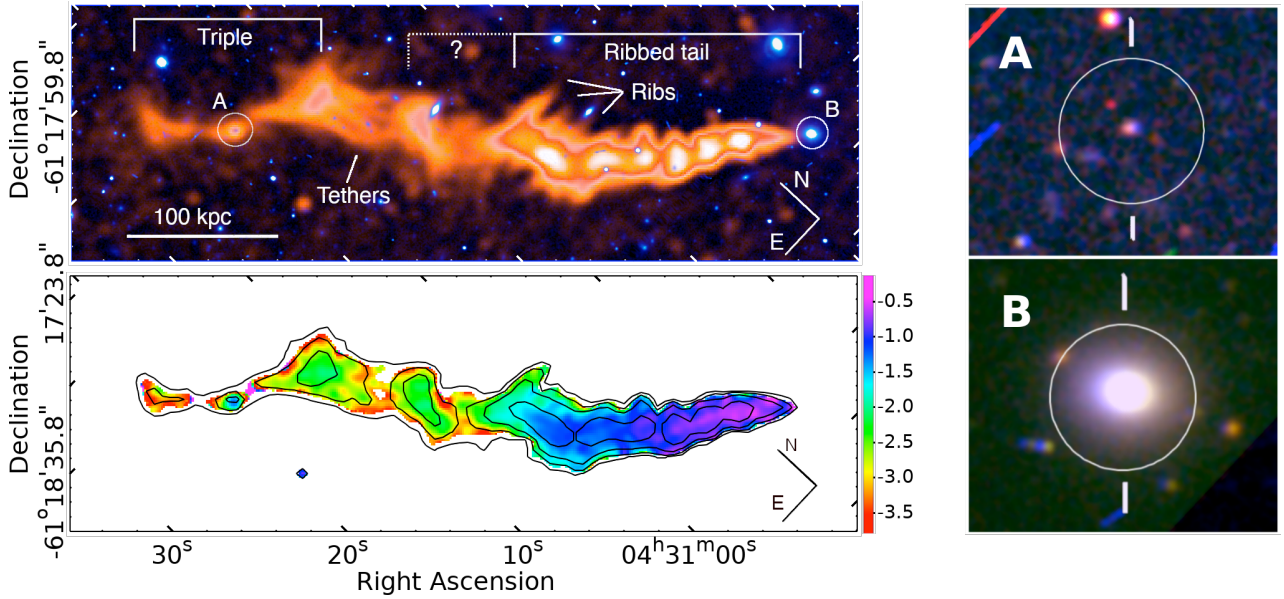

Fig. 19. Tailed radio source, *T3266*, NW of the centre of MCXC J0431.4−6126 (Abell 3266), which may be an extremely unusual composite of two independent sources. *Top left*: full-resolution (7.1″ × 6.7″) MGCLS Stokes-*I* intensity of the source (orange) overlaid on a DECam *g*-band image (blue). The radio brightness is on a non-monotonic scale, with the faintest regions of the tethers at ∼0.15 mJy beam^{-1} and the brightest regions at 2.2 mJy beam^{-1}. Circles, labelled A and B, indicate the positions of the two likely host galaxies (see the *right panels*). The physical scale at the cluster redshift is shown in the lower left corner. *Bottom left*: in-band spectral index map, with a strong steepening with distance from host B. *Right*: DECam *gri* composite images of the two proposed hosts labelled A and B in the top left panel. Host A is at RA = 04^{h}31^{m}18.48^{s}, Dec = −61°19′18.54″. Host B is at RA = 04^{h}30^{m}45.56^{s}, Dec = −61°23′35.8″.

between these two bright radio galaxies, some at lower brightness than visible in the images here. The origin of these structures is unknown.

Extensive networks of filamentary structure associated with a tailed radio galaxy are also seen in the LOw Frequency ARray maps of Abell 1314 (Fig. 25 in van Weeren et al. 2021). Ramatsoku et al. (2020) showed another spectacular example from MeerKAT observations of ESO 137−006, with 'collimated synchrotron' threads connecting the two radio lobes. The origin of all these features is still unknown. One speculative possibility mentioned by Parrish et al. (2012), Birkinshaw & Worrall (2015), and Donnert et al. (2018) is that there are pre-existing magnetic flux tubes in the ICM. Such features would become visible only when there was a sufficient population of relativistic electrons. Further spectral and polarisation work, and detailed comparisons with X-ray emission from the ICM will be needed to explain these novel phenomena.

7.5. A tail with ribs and tethers

At a distance of 350 kpc from the X-ray peak of Abell 3266 we identify a tailed radio galaxy (hereinafter *T3266*) with features not yet seen elsewhere, and whose physical origins are unclear. The structure appears in earlier maps by Bernardi et al. (2016) where it is shown to be elongated parallel to the cluster X-ray emission, positioned between the identified optical sub-clusters. The Abell 3266 galaxy cluster (listed in the MGCLS catalogue as J0431.4−6126) is likely in the midst of a complicated cluster merger, with an elongated X-ray distribution (Henriksen & Tittley 2002), two velocity-separated subclusters of optical galaxies in its core, and six sub-clusters on its peripheries (Dehghan et al. 2017). The cluster core has a mean redshift of 0.0594 ± 0.0005 and a velocity dispersion of 1460 ± 100 km s^{-1}.

The full-resolution MGCLS image of *T3266*, overlaid on the *g*-band DECam image, is shown in Fig. 19. *T3266* has a faint, 65 μJy beam^{-1} radio core (not visible in this image) associated with WISEA J043045.39−612335.6 (galaxy denoted by B in Fig. 19), at a redshift of 0.0626. The radio tail extends to the NE (from right to left in the figure), and the entire structure has a projected length of ∼6.7′ (∼480 kpc at the redshift of the presumed host). The region of the tail closest to galaxy B (the 'ribbed tail' in Fig. 19) shows distinct quasi-periodic changes in brightness and width. The tail is ∼20″ (23 kpc) wide at its half-intensity in this region, but its transverse profile is flat-topped and shows no signs of bifurcation. No other such features are seen in the MGCLS Abell 3266 field of view, and they are unlikely to be instrumental in origin. The four bright regions nearest the head of *T3266* are separated by ∼19″ (22 kpc), essentially the same as the jet width. This suggests that some instability in the flow may be regulating this behaviour. Some faint extensions transverse to the jet are also seen.

Farther back along the ribbed tail, three 'ribs' are clearly seen to extend perpendicular to the tail axis, with a full extent of up to 75″ (88 kpc). We speculate that they reflect some type of interaction with the external medium, or are related to the transverse structures seen in early numerical simulations of intermittently restarting jets (Clarke & Burns 1991). These unusual bright patches and ribs, with their periodicity and transverse extent, stand as a challenge for the current generation of magnetohydrodynamic numerical simulations of jets in a complex ICM.

It is also possible that the full structure of *T3266* may be a serendipitous projection of two separate sources, with the last 2′ of the tail (left-most in Fig. 19) potentially a separate triple source. The possible host of this source, indicated as galaxy A in Fig. 19, is a faint optical and infrared galaxy (DES J043118.45−611917.9 or WISEA J043118.50−611918.2)

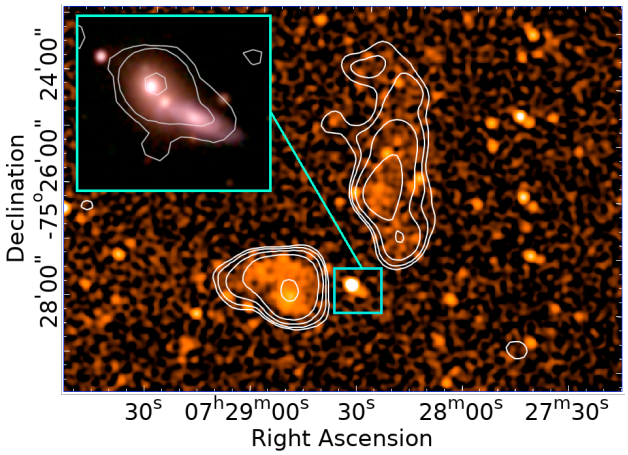

Fig. 20. Dying radio galaxy example, associated with WISEA J072832.45−752740.0, without detectable jets or hotspots in its diffuse lobes. The full-resolution (7.5″) MGCLS Stokes-*I* intensity image is shown in orange, overlaid with contours showing the filtered 25″ resolution intensity. It is outside of the primary-beam-corrected field of view of MCXC J0738.1−7506. The brightness (non-primary-beam-corrected) is on a logarithmic scale saturating at 0.1 mJy beam^{-1}, and contours are shown at 18, 24, 34, 54, 64 μJy/(25″ beam). The inset shows a zoomed-in view of a DECaLS image of the optical host, with full-resolution radio contours, that shows recent nuclear activity.

with a photometric redshift of 0.78 (Zou et al. 2019). If that identification is correct, the triple is a background giant radio galaxy, 900 kpc in length. The region between the ribbed tail and the triple, indicated by the dashed line in Fig. 19, and the three or more filamentary 'tethers', might belong to either source. They are each ∼50″ in projection, corresponding to 375 kpc and 58 kpc at the two redshifts.

It is not yet clear whether there are one or two individual radio galaxies in *T3266*, or even how to decisively answer that question. Either way, the tethers represent a new physical phenomenon, perhaps related to the collimated synchrotron threads of Ramatsoku et al. (2020) mentioned earlier. Unfortunately, the spectral index behaviour, seen in the bottom left panel of Fig. 19, does not provide a clear signature. In the region of the ribbed tail, *T3266* shows a monotonic spectral steepening with spectral indices ranging from −0.75 at the head to −1.4 in the region of the ribs. The spectra of the tethers appear very steep ($\alpha < -2$, though the spectral index is uncertain due to the low brightness of the region), and the triple source has spectral indices similar to the end of the tail, which is not expected if these are simply seen in projection.

7.6. Dying radio galaxies

One of the strengths of the MGCLS is in the detection of radio galaxies in their 'dying phase' (i.e. after the powering jets have been turned off). Studying such galaxies is important for understanding radio galaxy physics, the duty cycle of AGN activity, interactions with the surrounding environment, and for the usefulness of radio galaxies as cosmological probes. However, one needs a combination of high resolution (to ensure, within observational limits, that there are no significant hot spot regions or jets, and to identify the host galaxy), as well as good surface brightness sensitivity to detect the fading, dying lobes. Here we highlight two radio galaxies that might be in a dying phase of their lives, as examples of what is visible in the MGCLS data.

7.6.1. WISEA J072832.45−752740.0

The first example is shown in Fig. 20, and is associated with WISEA J072832.45−752740.0. At $z = 0.0138$ (Jones et al. 2009), this radio source is found serendipitously in the field of the $z = 0.111$ cluster MCXC J0738.1−7506. It has a total extent of ∼100 kpc, and the appearance of a wide-angle tail. Its luminosity of $\sim 10^{21}$ W Hz^{-1} is orders of magnitude below those of typical extended radio galaxies, although compact AGN emission at such low luminosities is more common (Lofthouse et al. 2018; Miller et al. 2009). The radio core, shown overlaid with a DECaLS image in the inset of Fig. 20, shows extended emission from likely interacting galaxies in a common envelope. We calculate minimum energy magnetic field strengths for each lobe, as 0.8 μG and 2 μG for the west and east lobes, respectively, assuming a spectral index of −1 and a proton/electron ratio of unity[15]. These imply radiative lifetimes of ∼70 Myr and ∼87 Myr, respectively, against a combination of synchrotron and Inverse Compton cooling. If the spectra were as steep as −2.5, the field strengths would increase by approximately a factor of 5, although the lifetimes would be similar, but now dominated by synchrotron losses. When the magnetic fields of dying radio galaxies drop below μG levels, the radio galaxies become very faint and the lifetimes become very short due to Inverse Compton losses (Rudnick 2004). The oldest, faintest sources will thus be rare and likely only be found in sensitive large area surveys.

7.6.2. Abell 548B

In our second example, the MGCLS provides a fresh look at Abell 548B[16]. The MGCLS images suggest that we are dealing with a large dying radio galaxy ∼14.2′ (650 kpc) in extent. The left panel of Fig. 21 shows the diffuse emission from this source at a resolution of 25″, overlaid on a false colour *gri*-composite Pan-STARRS image. The radio galaxy (B) is associated with a 6dFGS source, g0545049−254740, at a redshift of 0.036, almost 2000 km s^{-1} from the central cluster velocity. The radio core is itself double, as seen in the top right panel where red contours are from the Very Large Array Sky Survey (VLASS) 3 GHz map at 2.5″ resolution. This structure is similar to the classes of compact symmetric objects and medium symmetric objects (Conway 2002; Augusto et al. 2006), which are thought to be young objects. This similarity may be an indication of restarting activity for the large-scale radio galaxy, but the double structure is misaligned with respect to the large lobes, so the connection is unclear.

Embedded in the eastern lobe is a compact radio source (A) associated with the spiral galaxy 6dFGS g0545221−254730 at $z = 0.038$. It appears to have radio structures similar to those of a wide-angle-tail, swept towards the west by ∼80 kpc; it is not clear whether there is a physical connection to the dying radio galaxy as there is no obvious interaction with the diffuse lobe. At the western extremity, another spiral galaxy (C), likely unrelated, is seen in the radio. It is 6dFGS g0544374−255335 at $z = 0.039$. Finally, to the south, nearer the cluster centre, is a 220 kpc long narrow-angle tail, associated with 6dFGS g0545275−255510 (D) at $z = 0.042$. With their lower resolution and lower sensi-

[15] The source is at the edge of where we can make reliable primary beam corrections, and the S/N is low enough that the fluxes could be uncertain by up to ∼50%. This leads to an uncertainty of ∼12% in the derived fields, which is much lower than the uncertainties from the other assumptions.

[16] Abell 548B is the western component of what was originally classified as Abell 548, as described in Dressler & Shectman (1988).

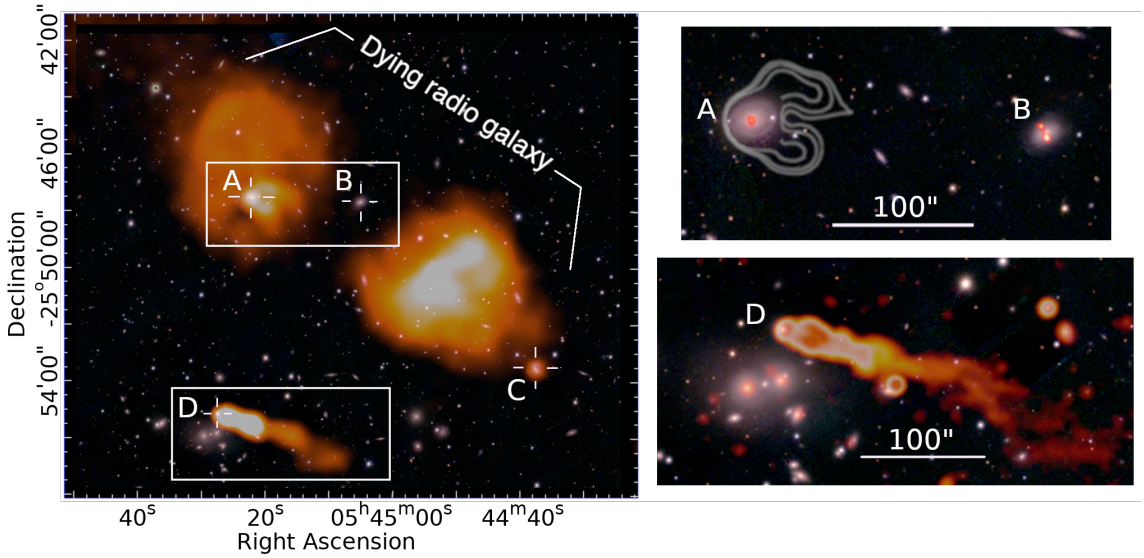

Fig. 21. A possible dying radio galaxy in Abell 548B. *Left*: diffuse emission filtered 25″ resolution MGCLS Stokes-*I* intensity image of Abell 548B (orange) overlaid on the false-colour *gri*-composite Pan-STARRS image. Previously misidentified structures (see Sect. 7.6.2 for details) are revealed to be a diffuse or dying radio galaxy to the north and a tailed radio galaxy to the south. The brightness scale is logarithmic, saturating at 1 mJy beam^{-1}. Radio sources A–D have clear optical counterparts, with B the likely host of the diffuse lobes and A a spiral galaxy embedded in the eastern lobe. *Top right*: zoomed-in view of the boxed region around sources A and B. White contours, showing the 15″ resolution MGCLS Stokes-*I* intensity at levels of (0.3, 0.35, 0.5) mJy beam^{-1} and edited for clarity, indicate tailed emission associated with the spiral galaxy, A. Red compact structures are from VLASS (Lacy et al. 2020) at 3 GHz with a resolution of 2.9″ × 1.8″ (p.a. 50°). The single VLASS component associated with A has a peak flux of 30 mJy beam^{-1}. There is a small double VLASS source associated with B, with a peak flux of 3.3 mJy beam^{-1}, indicating possible recent radio activity. *Bottom right*: zoomed-in view at full resolution (7.4″ × 7.4″) of the boxed region around the tailed source, D. The brightness scale is non-monotonic, and the peak brightness in the frame is 7 mJy beam^{-1}. 100″ corresponds to 84 kpc at the cluster redshift of 0.042.

tivity observations, Feretti et al. (2006) suggested that the radio galaxy lobes in the north and the diffuse emission to the south were instead merger-related relic structures outside of the bright X-ray region of the cluster. Now that MGCLS has elucidated the full structure of these sources, we recognise them as a combination of diffuse-lobed and tailed radio galaxies, as described above. We expect a closer examination of the MGCLS to unveil more, and fainter, examples of dying radio galaxies.

7.7. Bulk gas motions far outside clusters

The pair of radio galaxies shown in Fig. 22 provide an unusual, and perhaps unique, case of complex radio galaxy/medium interactions far beyond the cluster environment. Early on, tailed radio galaxies provided evidence of the relative motion of their host galaxies through the ICM (Miley 1980). More recently, modest excess radio galaxy bending has also shown the influence of such motions in local overdensities at >5 Mpc from the nearest cluster (Garon et al. 2019).

The two radio galaxies shown in Fig. 22 were found > 42′ from the centre of the $z = 0.0194$ cluster MCXC J1840.6−7709 (ESO 45−11). The northern source is associated with WISEA J184720.77−774444.2, at $z = 0.138$, and is therefore not associated with the cluster. The southern source is associated with WISEA J184722.38−774756.1, which has no available redshift; for the purposes of this discussion, we make the plausible assumption that the two radio sources belong to the same system. There are no other catalogued clusters in the vicinity, and no X-ray emission is visible in the ROSAT All-Sky Survey.

Multiple-bend sources such as these are important for understanding the dynamics of the diffuse, lower density thermal plasmas both in- and out-side of rich clusters. Simple relative

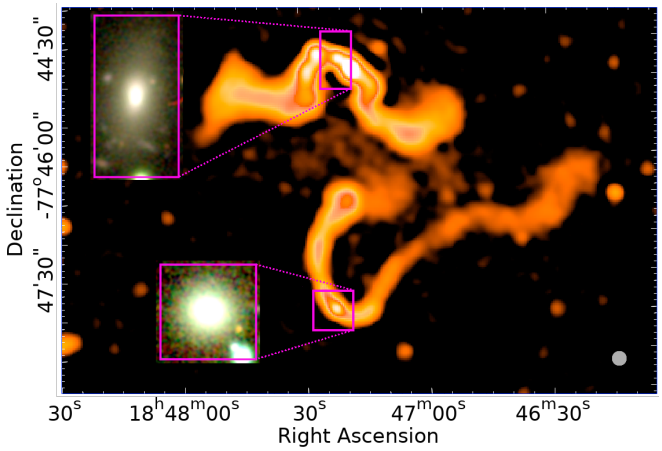

Fig. 22. Pair of radio galaxies with multiple bends found serendipitously in the MCXC J1840.6−7709 field, illustrating the likely effects of large-scale motions in the local external medium. The full-resolution (8.1″ × 7.6″) MGCLS Stokes-*I* intensity image is shown in orange, with a non-monotonic brightness scale and a peak flux of 13 mJy beam^{-1}. A false colour *zir*-composite DECam image of each host is shown in the insets. The MGCLS synthesised beam is shown in the lower right corner.

motions though an external medium would produce a C-shaped structure, but the bends in these sources require other external forces. The scale sizes are of the order of several hundred kiloparsecs. In order to see bends such as these, two factors are important. First, the irregularities in the external medium flows must be on scales comparable to the size of the radio galaxy;